Natural clay and biopolymer-based nanopesticides to control the environmental spread of a soluble herbicide

Natural clay and biopolymer-based nanopesticides to control the environmental spread of a soluble herbicide

Monica Granetto[(1)], Luca Serpella[(1)], Silvia Fogliatto[(2)], Lucia Re[(1)], Carlo Bianco[(1)], Francesco Vidotto[(2)], Tiziana Tosco [(1)(*)]

[(1)] DIATI – Politecnico di Torino, C.so Duca degli Abruzzi 24, 10129 Torino - Italy

[(2)] DISAFA – University of Torino, Largo Paolo Braccini 2, 10095 Grugliasco (TO) – Italy

[(*)] Corresponding Author: tiziana.tosco@polito.it

Submitted to

Science of the Total Environment

July 2021

Graphical Abstract

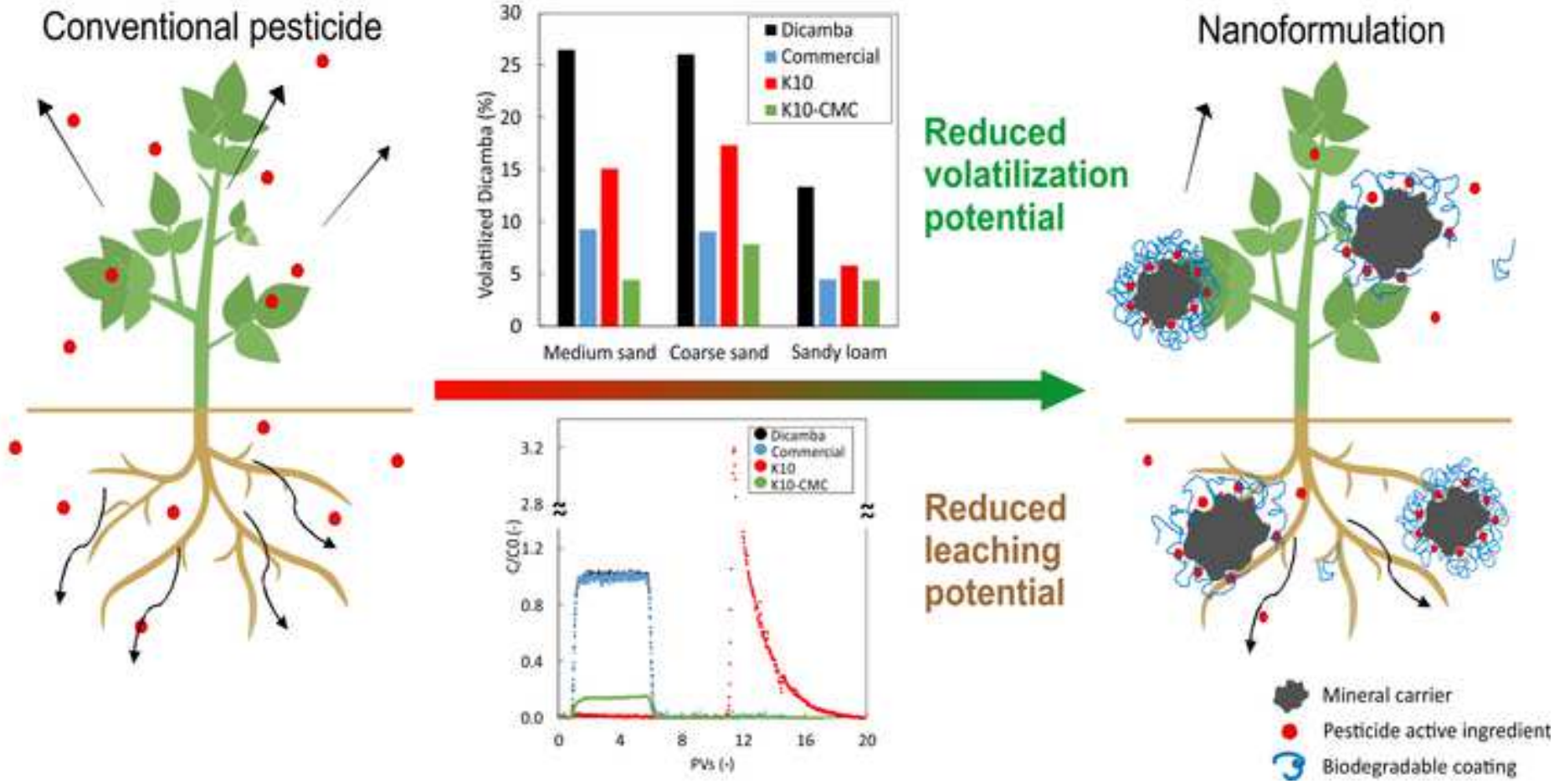

Highlights

natural clay and food-grade biopolymer are used in a novel nanopesticide formulation

natural clays showed effective in reduce environmental drawbacks of agrochemicals

the nanoformulation effectively encapsulated dicamba and controlled its release

the nanoformulation significantly reduced dicamba mobility in porous media

the herbicidal efficacy of dicamba was not hindered by the nanoformulation

Natural clay and biopolymer-based nanopesticides to control the environmental spread of a soluble herbicide

Monica Granetto[(1)], Luca Serpella[(1)], Silvia Fogliatto[(2)], Lucia Re[(1)], Carlo Bianco[(1)], Francesco Vidotto[(2)], Tiziana Tosco [(1)(*)]

[(1)] DIATI – Politecnico di Torino, C.so Duca degli Abruzzi 24, 10129 Torino - Italy

[(2)] DISAFA – University of Torino, Largo Paolo Braccini 2, 10095 Grugliasco (TO) – Italy

[(*)] Corresponding Author: tiziana.tosco@polito.it

Submitted to

Science of the Total Environment

July 2021

Abstract

Pesticides are essential in maintaining high crop yields. Their massive use is often associated to health and ecological drawbacks particularly noticeable for soluble and volatile pesticides, which are prone to significant dispersion in the environment. In this work a novel nano-formulation is proposed to control leaching and volatilization of a broadly used herbicide, dicamba. Dicamba is subject to significant leaching in soils, due to its marked solubility, and to significant volatilization and vapor drift, with consequent risks for operators and neighbour crops. Natural, biocompatible, low-cost materials were employed to control its dispersion in the environment: a nanosized natural clay (namely, K10 montmorillonite) was selected as a carrier to adsorb the pesticide, and carboxymethyl cellulose, a food-grade biodegradable polymer, was employed as a coating agent to control herbicide release. The synthesis approach is based on direct adsorption at ambient temperature and pressure, with a subsequent particle coating to increase suspensions stability and control pesticide release. The nano-formulation showed a controlled release when diluted to field-relevant concentrations, a volatilization comparable with commercially formulated products and a markedly reduced mobility in the porous medium compared to a commercial competitor.

Keywords

Nanopesticides, dicamba, controlled pesticide leaching, nanocarrier, natural clays

Highlights

- natural clay and food-grade biopolymer are used in a novel nanopesticide formulation
- natural clays showed effective in reduce environmental drawbacks of agrochemicals
- the nanoformulation effectively encapsulated dicamba and controlled its release
- the nanoformulation significantly reduced dicamba mobility in porous media
- the herbicidal efficacy of dicamba was not hindered by the nanoformulation

1. INTRODUCTION

The use of agrochemicals, including pesticides and fertilizers, is unavoidable for the optimization of crop production, but has numerous drawbacks on both human health and the environment (Damalas and Eleftherohorinos, 2011). Several products have toxic effects on aquatic life and beneficial insects, and a growing number of plant protection products have been found or suspected to be toxic or carcinogenic to humans. Herbicides are particularly relevant in this sense, being the agrochemicals most frequently found in superficial waters and groundwater. Many compounds have been banned from the list of authorized pesticides in most countries, and others are currently under evaluation. In Europe, the Regulation (EC) 1107/2009 has established a periodic assessment to renew the approval of active substances contained in pesticides to ensure that they continue to fulfill defined environmental and eco-toxicological criteria. In June 2021, only 463 out of 1454 substances that could be potentially included in pesticides (either as active substances, safeners or synergists) were regularly approved, while 61 are still under evaluation (European Commission, 2021).

The persistency, hydrophilicity, volatility and more in general the affinity of the individual substance to the different environmental matrices and components ultimately control their preferred migration routes and accumulation compartments, and consequently their long-term fate and associated potential risks for human health and ecological receptors. Poorly biodegradable substances tend to progressively accumulate in deep soil, sediments and groundwater, where they remain unaltered for years or even decades (Arias-Estévez et al., 2008; Wauchope, 1978). Consequently, pesticides prohibited several years ago still represent a significant threat for health and environment: as an example, about 7% of groundwater measurement stations in EU reported values exceeding the Environmental Quality Standards (EQS) levels in 2010 - 2011 for at least one agrochemical (Cyclodiene-group and Endosulfan) (EUROSTAT, November 2017; Lapworth et al., 2006), whereas at least one pesticidal compound was found in 83% of top soil samples collected across Europe (Silva et al., 2019).

Highly soluble compounds show a prominent infiltration potential with rain and irrigation (and consequently transport and accumulation in deep soil and groundwater is the preferred migration route), while volatile compounds are prone to significant dispersion in the atmosphere. It has been reported that 10% to 75% of the applied pesticides do not reach the target pest species (Aktar et al., 2009; Pimentel, 2009) and the unused product can therefore migrate towards non-target crops, insects and ultimately spread in the environment (Boutin et al., 2014; Sanchez-Bayo and Goka, 2014; van den Berg et al., 1999).

The major routes available to reduce the environmental impact of pesticides include the development of more efficient crop management strategies (Bongiovanni and Lowenberg-Deboer, 2004; Reichenberger et al., 2007), the identification of new, less toxic and less persistent substances with pesticidal effects (Dayan et al., 2009; Lamberth et al., 2013), and the development of new formulations of existing active ingredients (AIs) (Iavicoli et al., 2017; Sopeña et al., 2009). Nanotechnology can play an important role in finding new pesticide formulations with reduced toxicity and environmental impacts (Moulick et al., 2020; Servin et al., 2015; Worrall et al., 2018), even though research is still needed to verify several aspects of the actual efficacy and convenience of nano-formulated pesticides, particularly at the field scale (Gomes et al., 2019; Kah et al., 2018a; Singh et al., 2021; Usman et al., 2020). Nanopesticides consist of nanoparticles (NPs), usually referred to as nanocarriers, containing an active ingredient dispersed in a colloidal suspension. Nanopesticides are formulated with different objectives (Adisa et al., 2019; Kah et al., 2019; Kah et al., 2018b): to promote the use of AIs that are less harmful toward non-target organisms, but whose premature degradation may need to be hindered; to optimize pest targeting; to reduce the overall amount of employed chemical substances by improving the delivery of poorly soluble AIs, or conversely by controlling and retarding the release of soluble AIs. Two main types of nano-formulations are currently used: (1) NPs that act as pesticides themselves and (2) NPs that act as a carrier for AIs with pesticidal effects, adsorbed or immobilized on them using different techniques. With respect to this second class, both organic and inorganic formulations were developed. In the last few years, organic formulations, such as nanocapsules, nano- and microemulsions, and NPs with the AI incorporated in a polymeric matrix have become the most popular (Kah and Hofmann, 2014; Kah et al., 2018a).

In this work a nano-to-micro-formulation, aimed at reducing environmental spreading of a highly soluble and moderately volatile herbicide, namely dicamba (3,6 dichloro-2 methoxy benzoic acid), was developed. Dicamba is an auxin-like herbicide, registered in 1967, applied in post-emergence to control annual and perennial broadleaf weeds in non-agricultural settings, lawn and turf and in different crops, such as wheat, barley, corn, oats, millet, sorghum, and asparagus (Behrens et al., 2007). The principal metabolite is 3,6-dichlorosalicylic acid (DCSA), which showed moderate persistence and medium to slight mobility in the soil. Dicamba has been established to be toxic to aquatic organisms and its metabolite was defined as harmful (Authority, 2011). Because of its high efficacy, relative inexpensiveness, relative environmental safety and low risk for weeds to develop resistance, it is used worldwide. Dicamba, as well as other auxinic herbicides, is characterized by a high solubility, in the order of 6 to 8 g/l at ambient conditions, resulting in significant infiltration and consequent mobility in soil and subsoil (Oliveira Jr et al., 2001; Sakaliene et al., 2007) and relatively high volatility, with consequent drift problems and potential risks for users (Ding et al., 2019; Egan and Mortensen, 2012).

Natural materials were tested in this study for the development of the nano-formulation, namely mineral carriers (montmorillonite clays and a zeolite), and carboxymethyl cellulose (CMC) as a coating agent to minimize the loss of herbicide and modulate its release over time. It is known that mineral particulate matters such as silica and clay have a good affinity with a broad set of polar or ionizable pesticides, and have been successfully proposed as carriers in the development of nano-formulations. In most cases, natural particles are chemically modified to improve their affinity to the pesticidal molecule, such as in the case of organoclays (Cabrera et al., 2016; Cornejo et al., 2008; Hermosin et al., 2001). Synthetic hollow silica particles have also been successfully employed (Bueno and Ghoshal, 2020; Gao et al., 2020; Nuruzzaman et al., 2020). Less frequently, unmodified mineral particles have been directly used, e.g. montmorillonite for hexazinone (Celis et al., 2002), simazine and 2,4-D (Cox et al., 2000). The latter approach, even if often slightly less performing in term of loading capacity, was preferred in this work due to its higher sustainability and environmental compatibility, easier implementation and reduced cost.

Polymers, and in particular biopolymers, are currently used in the form of capsules (Petosa et al., 2017), polymeric microbeads and as a coating of solid carriers to control the release of encapsulated pesticides and fertilizers (Joshi et al., 2020; Shasha et al., 1976), protect labile compounds (Elhaj Baddar et al., 2020), and prevent excessive volatilization (Azeem et al., 2014; Dimkpa et al., 2020). Alginate is by far the most applied biopolymer (Kenawy and Sakran, 1996), even though carboxymethyl cellulose (Kök et al., 1999), lignin (Behin and Sadeghi, 2016), starches (da Costa et al., 2019), bio-based plastics (Riggi et al., 2011) and others have been employed.

In this work the efficacy and efficiency of four different natural mineral carriers, namely two Na-montmorillonites, a Ca-montmorillonite and a zeolite, as well as the opportunity of using a bio-polymeric coating to control the dicamba release were evaluated through different tests. The best performing formulation was identified based on a balance between technical constraints and potential environmental effects. The ideal nano-formulation should be the one showing the highest loading capacity (evaluated in terms of mass of dicamba adsorbed per mass of carrier), the highest colloidal stability in a broad range of hydrochemical conditions (to guarantee that the formulation can be diluted in water, usually tap water in real-scale applications without an abrupt aggregation and/or sedimentation of the carriers, which would hinder its use), the lowest release of dicamba after dilution, the lowest loss of dicamba due to volatilization (which represents one of the main environmental problems of this AI), the lowest mobility in the porous medium (thus limiting as much as possible the potential spreading of dicamba, if infiltrated with rain or intense irrigation), and obviously the most efficient in controlling weeds. Clearly not all these aspects – sometimes contrasting – can be maximized, and the optimal nano-formulation was identified as the most reasonable compromise.

2. MATERIALS AND METHODS

2.1. Materials

Four carriers, all provided in the form of dry powders, were tested: a K10 Na-montmorillonite (Sigma Aldrich, labelled K10 in the following), a generic Na-montmorillonite (Indigo Herbs, UK, labelled Na-M2), a Ca-montmorillonite (PraNaturals, UK, labelled Ca-M), and a zeolite (NaturaForte, Germany, labelled ZEO). A food-grade, low-molecular-weight carboxymethyl cellulose (WALOCEL® CRT30GA, Dow Chemical Company Ltd, US, labelled CMC) was tested as carrier coating.

Structure, shape and elemental composition of the carriers were investigated using SEM-EDS microscopy (JEOL, Japan) directly on the dry powders. The carrier particle size was determined using a disk centrifuge (DC24000 UHR, CPS, US). To this aim, the samples were dispersed in deionized water (DIw), allowed to hydrate, sonicated for 25 minutes prior measurement and analysed at a disc rate of 3000 rpm in the range 70-0.1 microns. The zeta potential of the four carriers dispersed in DIw (following the same preparation protocol) with addition of NaCl (1 mM to 100 mM) or $CaCl_2$ (0 to 1 mM) were determined with electrophoretic measurements using dynamic light scattering DLS (Zetasizer Nano ZSP, Malvern Instrument, UK).

Dicamba was provided by Alfa Chemistry (US). A commercial herbicide (Mondak 21 S, Syngenta, Italy) containing dicamba (not nano-formulated) at a nominal concentration of 243.8 g/l was used as a comparison in volatilization, transport and efficacy tests.

The tap water (TAPw) used for release and transport tests was drawn from the municipal water supply network and chemically analysed for salts, pH, EC and TDS (data reported in Supporting Information, Table S1).

A medium silica sand (Dorsilit 8, Dorfner, Germany; d_{10}, d_{50} and d_{90} equal respectively to 0.415, 0.45 and 0.5 mm), was used for volatilization and column transport tests. A coarse sand (Dorsilit 5G, Dorfner, Germany; d_{10}, d_{50} and d_{90} equal respectively to 1.12, 1.58 and 1.9 mm) and a sandy loam soil (collected at DISAFA - University of Torino, d_{10}, d_{50} and d_{90} equal respectively to 0.04, 0.065 and 0.148 mm) were used for

165 volatilization tests. For all sands, the granulometric curve (data reported in Supporting Information, Figure
166 S1) was determined via dry sieving, while real soil undergo to wet sieving.

167

168 2.2. Methods

169 2.2.1. Nanopesticide preparation

170 The carriers were loaded with dicamba using direct adsorption. Briefly, the carrier was dispersed in a dicamba
171 solution (in the range 0.125 g/L to 7 g/L). The suspensions were continuously mixed with a magnetic stirrer
172 in a closed vessel with reduced headspace to minimize volatilization. Contact times of 24 h and 2 h were
173 used. After loading, the suspensions were centrifuged and the precipitate was collected and stored as stock
174 nano-formulation.

175 Adsorption isotherms were determined for all tested carriers and loading conditions. After centrifugation,
176 the supernatant was filtered with a 0.45 micron syringe PTFE filter (Thermo Fisher Scientific, Waltham, USA)
177 and the dicamba concentration in the supernatant ($C_{w,eq}$ [M L^{-3}]) was evaluated via Uv-vis spectrophotometry
178 (Specord S600, Analytik Jena, Germany) at a wavelength of 280.5 nm (the calibration curve is provided in
179 Supporting Information, Figure S2). The adsorbed concentration, or adsorption capacity, expressed as
180 dicamba mass adsorbed per unit mass of carrier, $C_{s,eq}$ [M M^{-1}], was determined from $C_{w,eq}$ measurements via
181 mass balance.

182 In case of polymer-coated formulations, the CMC was added to the batch to reach a final polymer
183 concentration of 0.5 g/l. Polymer adsorption onto the loaded carrier was promoted via stirring for 2h.

184

2.2.2. Release tests

Release tests were conducted on all uncoated nano-formulations and on selected coated ones. All tested stock samples were obtained via loading of the carrier in a 7 g/L dicamba solution and with a contact time of 24 h, following the procedure described above.

The stock nano-formulation was dispersed in DIw or TAPw, depending on the tested condition, at a concentration of 5 g/L (1g of nano-formulation in 200 ml). The suspension was maintained in agitation with a magnetic stirrer at 200 rpm in a beaker sealed with parafilm, with reduced headspace to minimize volatilization, for at least 6 hours. Selected tests were prolonged to 30 h. A sample was periodically collected, filtered with a PTFE syringe filter to remove the carrier and analysed via spectrophotometry to determine the concentration of dicamba released from the nano-formulation.

The fraction of herbicide retained on the carrier at a given time, R(t), was evaluated as:

$$R(t) = 1 - \frac{C_w(t) \cdot V_w(t)}{C_{s,eq} \cdot M_{s,C}} \qquad \text{(eq. 1)}$$

where $C_w(t)$ is the dicamba concentration measured in the water sample collected at time t [M L^{-3}], $V_w(t)$ is the dispersion volume at time t [L^3], $C_{s,eq}$ is the adsorbed concentration at the beginning of the test, and $M_{s,C}$ is the dry mass of carrier present in the system at the beginning of the test [M].

2.2.3. Volatilization tests

Volatilization tests were performed for uncoated and CMC-coated K10 nano-formulations (labelled respectively K10 and K10-CMC) and compared with a pure dicamba solution and with the commercial product. All samples were diluted in DIw in order to reach the same concentration of the AI (3 g/l).

In pre-screening tests, direct volatilization from the solution/suspension was assessed. Each sample was exposed to ambient air on a petri dish (Mueller, 2015; Strachan et al., 2010), which was periodically weighted for 30 hours. Tests were run at least in duplicate, at ambient temperature. After 30 hours the remaining mass

of dicamba was determined via solvent extraction method: acetonitrile and water at a mass ratio of 7:3 were added and kept in agitation for 24h in a closed vial with minimal headspace; the solution/suspension was then filtered using a PTFE syringe filter and analysed with UV-vis spectrophotometry. Two blank sets of tests containing only K10 and one with only water were run to check possible releases from sand and carriers that may interfere with the UV-vis analysis (no interference was observed).

Volatilization from dicamba-sprayed soil was then assessed in a second set of tests. The coarse and medium sands and the sandy loam soil were air-dried; the soil was sieved to remove particles and conglomerates larger than 2mm. 15 g of soils were added to each petri dish, sprayed and treated similarly to the pre-screening tests. Blank tests that included soil only (no spray), soil sprayed with water only and soil sprayed with K10 suspension (no dicamba) were run in parallel.

2.2.4. Column transport tests

Column transport tests in saturated conditions, aimed at mimicking carrier and pesticide transport in groundwater, were performed for K10 without pesticide loading (with or without polymeric coating), pesticide-loaded K10 (with or without coating), pure dicamba solution and the commercial product. Pre-screening tests with carrier only (with and without coating) were also run.

A Plexiglas column with adjustable ends and internal diameter of 1.6 cm was wet-packed with 36.5 g of Dorsilit 8 sand to an average length of 11.61 (±0.15) cm. The sand was hydrated and degassed prior packing to remove residual air microbubbles. A polypropylene filter with 120 μm mesh was placed at the top and bottom of the column to avoid sand from entering inlet and outlet tubing. The solutions/suspensions were injected in saturated conditions with a peristaltic pump (ISMATEC REGLO Analog MS-4/8, Cole-Parmer, Germany) at a constant flow rate of $1.46 \cdot 10^{-8}$ m^3/s, corresponding to a Darcy velocity of $7.26 \cdot 10^{-5}$ m/s. Inflow and outflow concentration of solutes and suspensions was monitored via optical density measurements using the UV-vis spectrophotometer equipped with from-through quartz cells with 5 mm lightpath (Hellma,

Germany). Monitoring wavelengths of 198.5 nm, 280.5 nm and 350 nm were adopted for NaCl, dicamba and carriers, respectively (calibration curves in Supporting Information, Figures S2 and S3). For tests involving the nano-formulations, outflow samples were also manually collected, filtered and analysed to reconstruct the breakthrough curve of free dicamba.

The nano-formulations were injected at a carrier concentration of 0.9 g/l, corresponding to a dicamba concentration of approximately 50 mg/l (the actual concentration slightly varied based on the specific tested formulation). This concentration corresponds to approximately 10% of the typical recommended concentration for dicamba-based products when applied on weeds: after field applications the most commonly detected dicamba concentration in leaching water is 3% to 10% of the applied one (Sakaliene et al., 2007; Tindall and Vencill, 1995), and consequently the most severe expected scenario for groundwater contamination was adopted.

Preliminary transport tests of K10 alone (without dicamba loading), with and without CMC coating, followed this protocol:

1. Pre-equilibration with DIw for at least 5 pore volumes (PVs)
2. Tracer injection (NaCl 30 mM) for 5 PVs
3. Flushing with DIw for 5 PVs
4. Injection of K10 dispersed in DIw for 5 PVs
5. Post-flushing with DIw for at least 5 PVs

The injection protocol for pesticide transport tests (including dicamba solution, nano-formulations and commercial herbicide) included the following steps:

1. Pre-equilibration with DIw for at least 5 PVs
2. Pre-flushing with background electrolyte solution (NaCl 30 mM) or TAPw (depending on the specific test) for 5 PVs
3. Injection of the dicamba solution/nano-formulation (dispersed in NaCl 30 mM solution or in TAPw) for 5 PVs

4. Post-flushing with NaCl 30 mM solution or TAPw for 5 PVs
5. Second post-flushing with DIw for at least 5 PVs

The porosity and the dispersivity coefficient of the sand-packed columns were determined for each transport tests by least-squares fitting the NaCl breakthrough curve (i.e. steps 1 and 2 of the injection protocols) to the classic advection-dispersion partial differential equation for conservative solutes:

$$\varepsilon \frac{\partial C_t}{\partial t} = -q \frac{\partial C_t}{\partial x} + \alpha_x \frac{\partial^2 C_t}{\partial x^2} \quad \text{(eq. 2)}$$

where C_t is the tracer concentration [M L^{-3}], q is Darcy velocity [L T^{-1}], ε is the effective porosity [-] and α_x is the dispersivity coefficient [L] of the porous medium.

The transport of the carriers was modelled using the modified advection-dispersion-deposition equation usually adopted to describe colloid transport in saturated porous media:

$$\begin{cases} \varepsilon \frac{\partial C}{\partial t} - \sum_i \rho_b \frac{\partial S_i}{\partial t} = -q \frac{\partial C}{\partial x} + \alpha_x \frac{\partial^2 C}{\partial x^2} \\ \rho_b \frac{\partial S_i}{\partial t} = \varepsilon k_{a,i} \left(1 + A_i S_i^{\beta_i}\right) C - \rho_b k_{d,i} S_i \end{cases} \quad \text{(eq.3)}$$

where C is the carrier concentration in water [M L^{-3}], S_i is the concentration of carrier particles retained on the solid grains due to the i-th retention mechanism [M M^{-1}], ρ_b is the bulk density of the porous medium [M L^{-3}], $k_{a,i}$ is the carrier attachment rate due to the i-th retention mechanism [T^{-1}], $k_{d,i}$ is the corresponding detachment rate [T^{-1}], A_i and β_i are empirical coefficients specific to the deposition mechanism [-].The first equation refers to particle transport in water and the second one describes the deposition mechanism(s). The parenthesis in the second equation is the generic formulation for particle retention mechanisms proposed by Tosco and Sethi (Tosco and Sethi, 2010). For linear attachment, $A_i = \beta_i = 1$; for blocking, $\beta_i = 1$ and $A_i = -1/S_{max,i} < 0$ (where $S_{max,i}$ is the maximum concentration of particles retainable on the solid matrix due to the i-th retention mechanism); for ripening, $A_i > 0$ and $\beta_i > 0$. In case of irreversible deposition, the second term vanishes being $k_{d,i} = 0$.

In this work the following two-site deposition model was adopted:

279
$$\begin{cases} \varepsilon \frac{\partial C}{\partial t} - \rho_b \frac{\partial S_1}{\partial t} - \rho_b \frac{\partial S_2}{\partial t} = -q \frac{\partial C}{\partial x} + \alpha_x \frac{\partial^2 C}{\partial x^2} \\ \rho_b \frac{\partial S_1}{\partial t} = \varepsilon k_{a,1} C \\ \rho_b \frac{\partial S_2}{\partial t} = \varepsilon k_{a,2} \left(1 + A_2 S_2^{\beta_2}\right) C \end{cases} \quad \text{(eq. 4)}$$

280 The breakthrough curves of tracer and particles were inverse-fitted to the respective transport equations
281 using the software MNMs 2018 (Micro-and Nanoparticle transport, filtration and clogging Model - Suite)
282 (Bianco et al., 2016; Mondino et al., 2020; Velimirovic et al., 2020). A porosity of 0.31 (±0.02) and dispersivity
283 of $1.84 \cdot 10^{-4}$ ($\pm 3 \cdot 10^{-7}$) m were obtained from tracer tests, and were assumed valid also for particle transport,
284 since no evidence of particle early breakthrough was observed.

285 Dicamba adsorption/desorption onto/from the carriers was not modeled since all nano-formulations were
286 prepared for injection a few hours in advance, thus allowing the complete release of the pesticide before
287 injection into the column.

288

289 ### 2.2.5. Weed control efficacy tests

290 Weed control efficacy of the commercial dicamba, K10 and K10-CMC was evaluated in greenhouse on
291 *Solanum nigrum* and *Amaranthus retroflexus*, two dicamba sensitive weeds, grown in pot filled with
292 commercial potting mix. Each pot contained 5 seeds of a single weed species and 4 replicate pots were
293 prepared for each combination of herbicide formulation, dose and species. The experiment was repeated
294 twice, in May and August 2019. When weeds reached a two to three leaf stage, they were sprayed with the
295 following equivalent dose of dicamba: 0 (untreated control), 146.3, 195.0, 219.4, 243.8, 268.2 and 292.6 g AI
296 ha^{-1}, corresponding to the following volume of commercial dicamba: 0, 0.6, 0.8, 0.9, 1 (field rate), 1.1. and
297 1.2 L ha^{-1}. Seedrape oil (Codacide, Corteva) used at 1 L ha^{-1} as an adjuvant was added to all the spray solutions.
298 Herbicide treatment was performed using a cabinet sprayer equipped with a single flat fan nozzle (Teejeet
299 AI11002-VS), calibrated to deliver 300 L ha^{-1} at a pressure of 203 kPa. After treatment, pots were randomly
300 arranged in greenhouse benches until the study ended. At 21 days after treatment the fresh biomass of
301 treated plants was weighted by cutting them just above the soil level. Treatment efficacy was expressed as

302 percentage of fresh aboveground weight relative to the untreated control (relative weight %). Values of
303 relative weight may range from 0% (complete plant desiccation) to 100% (fresh weight of untreated plants).

304 A dose-response curve was built for each herbicide formulation, averaging between experiments, separately
305 per weed species. The percentage of relative weight of treated plants was fit against herbicide rates
306 according to a three-parameter log-logistic regression model (Equation 5):

307 $$Y = \frac{d}{1+exp\{b[log(x)-log(e)]\}} \quad \text{(eq. 5)}$$

308

309 where *Y* is the relative weight of treated plants, *x* is the herbicide rate expressed in g AI ha^{-1}, *d* is the upper
310 limit, and *b* is the relative slope at the point of inflection *e*. Model fitting was performed using the *drm*
311 function of the DRC add-on package of the open-source program R (Fogliatto et al., 2021; Team\, 2019). The
312 effective herbicide dose required to reduce plant relative weight by 50% (ED_{50}) and 90% (ED_{90}) compared
313 with the values observed at 0 g AI ha^{-1} were calculated from the fitted model using the *ED* function of the
314 DRC package.

315

316 3. RESULTS AND DISCUSSION

317 3.1. Carrier characterization

318 Information on particle size, zeta potential and fraction of retained herbicide after dilution was used to
319 identify the best performing carrier and coating, to be further assessed in the following steps of the study.

320 The particle size distribution was measured for the carriers dispersed in deionized water using a disk
321 centrifuge (Supporting Information, Figure S4). Table 1 reports the D_{10}, D_{50} and D_{90} values obtained for all
322 samples from the cumulated particle size distribution. D_{50} is in the range 0.5 - 2.5 μm for all samples. The
323 particles are broadly distributed, with uniformity coefficient above 4 in all cases, and show a dominant

fraction in the micrometer range, and a secondary fraction in the nanometer range. In particular, a wide peak in the range 2 - 4 μm was observed for all materials except the zeolite (ZEO), which showed a wider peak in the range 3 - 10 μm. Only the Na-M2 sample showed a clear second peak, around 200 nm.

The zeta potential (Supporting Information, Figure S5) of the carriers was negative in all explored conditions, as expected for clays and zeolites. More negative values were measured for particles dispersed in DIw; when particles were dispersed in NaCl or $CaCl_2$ solutions at a high salinity, the zeta potential approached zero, suggesting lower colloidal stability. It is worth to highlight that Ca-M particles showed, in all solutions, zeta potential values closer to neutrality compared to the other particles, suggesting that they may be more prone to aggregation. This was confirmed by a general tendency of Ca-M to sediment faster when dispersed in solutions other than DIw (including tap water). Such a fast sedimentation rate, visible even by eye, cannot be attributed to a difference in size of primary particles nor to a higher density. This behaviour compromised the use of Ca-M in some tests, as discussed in the following paragraphs.

3.2. Adsorption and release tests

The capability of the four candidate carriers to adsorb the pesticide was evaluated first based on adsorption isotherms. To this aim, carriers were loaded with dicamba, in the absence of polymeric coating, in a broad range of herbicide concentration (0.125 g/L to 7 g/L). The upper concentration limit was selected close to the dicamba solubility (8 g/L at pH 1.9).

A contact time of 24 h was first selected based on the literature (Azejjel et al., 2009; Carrizosa et al., 2001). The adsorption isotherms (Figure 1) showed a linear relationship between adsorbed and dissolved herbicide concentration (respectively $C_{s,eq}$ and $C_{w,eq}$) in the explored concentration range. Thus, experimental data were fitted with a linear isotherm, $C_{s,eq} = K_d \cdot C_{w,eq}$. All carriers reached the highest loading capacity for the highest tested concentration. Comparing carriers, the calcium montmorillonite (Ca-M) and one of the sodium montmorillonites (Na-M2) reached the highest loading capacities, corresponding to adsorbed concentrations

348 of approximately 120 mg of dicamba per gram of carrier in both cases. The fitted partition coefficients are,
349 respectively, 0.0251 L/g (R^2 = 0.9759) and 0.0216 L/g (R^2 = 0.9966). The K10 sodium montmorillonite reached
350 a maximum of 80 mg/g, with K_d = 0.0124 L/g (R^2 = 0.9612); the lowest loading capacity was registered for the
351 zeolite (ZEO), which showed a maximum retained dicamba mass of 62 mg/g, with K_d = 0.0122 L/g (R^2 =
352 0.9893).

353 A shorter contact time (2 h) was also tested in view of a possible optimization of the loading procedure.
354 However, the results were not univocal (Supporting Information, Figure S7), showing for Ca-M a loading
355 capacity comparable to the one obtained in 24 h, a slightly higher $C_{s,eq}$ for K10, and lower for Na-M2 and ZEO.
356 The results were only partly reproducible, thus suggesting that for at least some carriers a contact time of 2
357 hours does not guarantee equilibrium between phases. In particular, the structure of zeolite, characterized
358 by cages and channels between the structural tetrahedral that form the primary porosity, is likely responsible
359 for the lowest performance of the ZEO sample at short contact time (Rhodes, 2010; Stocker et al., 2017).
360 Based on adsorption isotherms, a contact time of 24 h was therefore adopted for the following steps of the
361 study, for all carriers.

362 Release tests were carried out diluting the nano-formulations in DIw or TAPw, the latter to simulate
363 conditions similar to real pesticide application in the field. The nano-formulation concentration after dilution
364 (5 g/l) corresponded to a dicamba concentration of 0.42, 0.58, 0.55 and 0.34 g/l, respectively for K10, Na-
365 M2, Ca-M, ZEO (compare to adsorption isotherms). This dilution ratio was selected appropriately to
366 guarantee a dicamba concentration in the range of recommended application rate of the commercial
367 products (namely 0.12-1.46 g/l of dicamba, depending on the specific crop).

368 Release tests in DIw (Figure 2a) were used as a screening for the selection of the best candidate carrier, in
369 combination with adsorption and characterization results. When the uncoated nano-formulations were
370 diluted in DIw, Na-M2 showed the lowest percentage of retained pesticide, both on the short term (less than
371 1 hour) and on a longer time frame (60 hours and later). The highest release was observed in less than 1 hour,
372 with a subsequent partial re-adsorption on later stages. A final percentage of approximately 30% of dicamba
373 retained on the Na-M2 carrier after dilution was registered for the uncoated carriers, and similar results were

obtained also for the CMC-coated carrier (data not reported). This result indicates that Na-M2, even if capable to perform better than other carriers in terms of adsorption capacity, is not a suitable candidate for the dicamba nano-formulation. Even if a high release in a short time could be desirable for applications where an initial higher herbicide quantity is required, in light of the high dicamba volatility a Na-M2 based nano-formulation would not be the optimal choice because of the high risk of pesticide losses in air.

Ca-M showed the highest percentage of retained pesticide after dilution in DIw (approximately 80%). However, a peculiar behaviour was observed for this carrier: a fast, significant release was registered on a short time frame (1 h), leading to a retained percentage of 65%. In a longer time frame, part of the pesticide was re-adsorbed, leading to a final percentage of 80% retained dicamba approximately two hours after dilation. Based on high retention only, Ca-M would have been the best candidate carrier for the development of the nano-formulated dicamba. However, the high variability over time of the retained dicamba may lead to a partly unpredictable behaviour at the field scale: it is not possible to assume a priori how much time would it take for a farmer to start the field application of the pesticide after its dilution. If this time is shorter than one hour, it is possible that a high fraction of AI is dissolved in water, and therefore prone to volatilization and/or free infiltration in the subsoil. Moreover, its relatively poor colloidal stability, highly sensitive to salt content even in the presence of a polymeric coating, weakens its suitability for real-scale applications, where ionic strength and salt composition of natural or tap water used for pesticide dilution is not under control and highly variable. In light of these considerations, Ca-M was not further considered in the development of the dicamba nano-formulation.

ZEO and K10 showed similar behaviours, with approximately 55% of dicamba remaining adsorbed on the carrier 6 hours after dilutions, therefore resulting suitable candidate carriers. However, due to the higher adsorption capacity of K10 compared to the zeolite, K10 was selected as the best candidate for the next steps of the study. It is also worth to mention that the K10 carrier showed the most constant trend in dicamba release, with an initial fast release in the first 10 minutes, followed by a fast stabilization.

The polymeric CMC coating helped reducing the dicamba release from K10: CMC-coated particles diluted in DIw (Figure 2b) showed a fast (less than 10 mins) stabilization on a plateau corresponding to approximately

80% of retained dicamba, comparable with uncoated Ca-M, with an overall increase of retained AI of approximately 25% with respect to the uncoated K10. The coating is expected to primarily act by hindering the herbicide desorption, increasing the diffusive path toward the bulk fluid(Rashidzadeh et al., 2017). Conversely, when the nano-formulations were diluted in TAPw, the effect of the CMC coating on the release was reduced (Figure 2b), particularly on the long term: the released dicamba was 28% after 6h from both formulations, with a slightly higher release for the coated formulation in the first 3 hours. The major elements expected to influence the release behaviour are pH and salt content. The pH of the formulations diluted in tap water was 8.4 and, since dicamba has a very low pK_a (pK_a=1.95), in this alkaline environment the herbicide is present primarily as a deprotonated species; the presence of ionic species in water, such as HCO_3^- and PO_3, could inhibit the release from the clay surface when coating is not present.

3.3. Volatilization tests

Pre-screening volatilization tests were performed exposing to ambient air the diluted K10-based nano-formulations (K10 and K10-CMC), pure dicamba solution and diluted commercial product on petri dishes, without soil. The results (Supporting Information, Figure S8) showed a marked volatilization of pure dicamba: after 24 hours about 30% of the AI was lost via volatilization, indicating a moderate attitude of the AI to pass in air phase. Volatilization from the commercial product was negligible, with 99.7% of the pesticide mass remaining after 24 hours, likely thanks to the co-formulants, aimed, among other purposes, at increasing wettability and adhesive performance of the formulated dicamba, thus reducing water-air mass exchange. The uncoated K10 formulation, despite the high amount of AI released in water, limited the volatilization losses to 7.6% of the initial dicamba mass. Interestingly, a simple mass balance suggests that the presence of the K10 particles in the solution inhibits also the volatilization of the freely dissolved dicamba: for uncoated nano-formulations diluted in DIw, approximately 45% of the dicamba initially adsorbed on the carrier is expected to be released after dispersion in DIw (based on release tests), 30% of which should in principle be lost via volatilization (based on pure dicamba volatilization results). However, this would correspond to an

425 overall volatilization of 13.5% of the initial dicamba mass, while only 7.6% was observed here. This could be
426 linked to the specific experimental configuration (i.e. concentrated formulation applied on a petri dish): the
427 rapid water evaporation (expected to occur the first 1h of the test) may have left the AI in contact with the
428 air phase, with higher mass exchange in the first phase of the test; later on, tortuous paths can have formed
429 through the clay film over the petri dish while water was evaporating, with an overall reduced contact
430 between dissolved dicamba and air. However, more interestingly, it is also possible that, during water
431 evaporation, part of the dissolved dicamba re-adsorbed onto the clay particles due to the altered equilibrium
432 between the phases (Sciumbato et al., 2004; Strachan et al., 2010). At this stage it is not possible to
433 discriminate between the two processes and, likely, the observed results are obtained as a combination of
434 both. For the CMC-coated formulation a similar trend was observed, with even more limited volatilization,
435 resulting in an overall loss of 4.6% of the initial dicamba mass after 30 hours, thus confirming the usefulness
436 of the polymeric coating also to prevent volatilization(Rashidzadeh et al., 2017).

437 The dicamba formulations applied to soils evidenced similar volatilization trends (Figure 3). As a general rule,
438 dicamba alone showed the highest losses: in medium and coarse sand the volatilization was very similar, with
439 approximately 26% of AI losses in 24h; in sandy loam, the volatilization rate was lower (13.4%). Also for the
440 commercial formulation and for the two nano-formulations, the volatilization was more pronounced in the
441 sand samples and reduced in the sandy loam, suggesting a partial affinity of the compound to the fine fraction
442 of the soil. Contrary to the preliminary volatilization tests performed assessing direct volatilization from the
443 solution, when applied to soils the commercial formulation and the CMC-coated nano-formulation showed
444 comparable volatilization rates. In coarse sand and sandy loam the AI loss is respectively close to 8% and
445 4.5%, while in medium sand the coated nano-formulation performed significantly better than the commercial
446 dicamba-based product, showing a loss of 4.5% versus 9.3%. It is finally worth to highlight that in all cases,
447 but particularly in the two sand samples, the presence of the CMC coating significantly reduced the dicamba
448 volatilization (from 15.1% to 4.5% in medium sand, from 17.4% to 7.9% in coarse sand, and from 5.8% to
449 4.5% in sandy loam), thus confirming the key role of the polymeric coating in controlling the release of
450 dicamba from the montmorillonite carrier.

3.4. Transport in the porous medium

Preliminary transport tests were performed injecting the K10 carrier with and without the polymeric coating in sand-packed columns to assess the potential role of the polymeric shell in modifying particle transport. In DIw the presence of the CMC coating is not expected to play a significant role in particle transport. The zeta potential of both coated and uncoated particles is strongly negative (-25.2±0.46 mV for uncoated K10, -38.4±0.89 mV for CMC coated K10). To help understanding transport-controlling processes, DLVO interactions were estimated (Elimelech, 1995). Both particle-particle and particle-sand DLVO interaction profiles are repulsive without secondary minima, which could suggest mild aggregation and/or deposition (Supporting Information, Figures S9a and S10a). Coherently, the particle breakthrough curves (BTCs) obtained from column transport tests (Figure 4) show a non-negligible mobility of both coated and uncoated carrier. In both cases the breakthrough concentration approached 60% of the injected one, showing minimal influence of the coating. The mass balance (Table 2) indicates a slightly higher mobility for the CMC-coated particles, coherently with slightly more repulsive particle-particle and particle-collection DLVO profiles: 67.22% of the injected mass of coated K10 was eluted at the end of the test, while 63.09% was recovered at column outlet for bare K10. Based on the measured zeta potential values and the clearly repulsive DLVO interaction it is possible to attribute the carrier retention in the porous medium mainly to physical mechanisms, above all to mechanical filtration: the K10 particles, even if stably dispersed in the injected suspension, are sufficiently large to partly interact with the porous medium; the ratio of K10 d_{90} (3.746 µm) to sand d_{10} (370 µm) approaches the critical ratio of 1% above which a partial mechanical filtration of particles can be observed (Luna et al., 2015; Xu et al., 2006). The experimental breakthrough curves were modelled using a dual deposition site attachment/detachment model (eq. 4) with a linear irreversible deposition site (representing mechanical filtration) and a linear reversible deposition site (representing physical-chemical interactions, obtained imposing $A_2 = 0$ in the model equation). They showed a good agreement between simulated and measured BTCs. The fitted coefficients are reported in the first two columns of Table 2. The

476 first interaction site is dominant, thus reflecting the dominance of mechanical filtration as retention
477 mechanism. The particle retention observed in these tests can be assumed to be the minimum to be
478 reasonably expected in all experimental conditions, due to the clearly repulsive interactions.

479 When comparing the different dicamba-based formulations dispersed in NaCl 30 mM solutions (Figure 5), a
480 significant discrepancy between nano-formulated and not nano-formulated suspensions is observed. Pure
481 dicamba and the commercial product, as it can be denoted from their breakthrough curves, were transported
482 similarly to a trace. They reached $C/C_0 = 1$ with no evident delay (thus indicating the absence of any relevant
483 adsorption phenomenon onto the silica sand) and all injected mass is recovered at column outlet at the end
484 of the test (recovered mass of 99.35% for pure dicamba and 98.44% for the commercial product).

485 The K10-formulated dicamba, both in presence and absence of coating, showed a remarkably limited mobility
486 compared to pure and commercial dicamba. During the injection and subsequent flushing at constant NaCl
487 concentration (i.e. in PVs 1 to 10), the uncoated formulation did not show any appreciable breakthrough,
488 while the CMC-coated formulation reached a maximum outflow concentration equal to 15.3% of the injected
489 one (Figure 5, respectively red and green curves). In terms of mass balance, this corresponds to 1.74% of
490 injected uncoated K10 nano-formulation reaching the column outflow and 14.45% of the coated one in the
491 first PVs. The breakthrough curves of the two carriers were successfully fitted with eq. 4 (Supporting
492 Information, Figure S11). In this case the fitted attachment coefficients for site 1 (linear irreversible
493 attachment) are approximately one order of magnitude higher than those obtained for the carriers in DIw,
494 both for coated and bare K10, indicating that a stronger physical retention was occurring for the nano-
495 formulations dispersed in the NaCl solution compared to the carriers dispersed in DIw. As for the second
496 interaction site, for the CMC-coated K10, a linear reversible interaction ($A_2 = 0$) was adequate to represent
497 the physical-chemical interaction, while for the bare particles a ripening mechanism ($A_2 > 0$) correctly
498 described the particle physical-chemical interactions occurring in the porous medium. This is in agreement
499 with the predicted DLVO interaction profiles (Supporting Information, Figures S9b and S10b): for the CMC-
500 coated nano-formulation, a weakly repulsive profile is obtained for particle-particle interaction, with a
501 shallow secondary attractive minimum and a very limited energy repulsive barrier (~0.2 KT), suggesting that

aggregation may partly occur in the suspension. Conversely, for the uncoated K10 formulation, an entirely attractive profile is obtained, indicating that particles are attracting each other and agglomerating. As for particle-collector interaction, on the contrary, repulsive profiles are observed, even though the repulsive energy barrier against deposition is of limited extent (~2-4 KT). In terms of particle part transport, this suggests that, for the uncoated formulation, particles are partly aggregated, thus prone to a more pronounced mechanical filtration (represented by the first interaction site) with respect to the carrier in DIw, and deposited particles are attracting suspended ones, thus resulting in a strong ripening (reflected by the second interaction site). For the coated nano-formulation, the CMC shell prevents excessive aggregation, mechanical filtration is more limited and ripening does not occur, at least on the time scale and travel path explored in these tests.

It is worth to recall that, when the nano-formulations are diluted in water, a fraction of dicamba is released and therefore is present as freely dissolved compound in the injected suspensions; in these tests this fraction corresponded approximately to 25% of the total dicamba for uncoated K10 and 20% for CMC-coated K10 (compared with release tests). The breakthrough curves for the free fraction of dicamba (Supporting Information, Figure S12) show that, for both nano-formulations, the free compound is transported through the sand-packed column similarly to a tracer, with no evidence of any retention. Based on this additional information, it is possible to draw a mass balance for the total dicamba (i.e. both freely dissolved and embedded in the carrier), which indicates that, at the end of the first 10 PVs, for the uncoated carrier 10% of the injected dicamba has been eluted from the column, and 20.73% has been eluted for the CMC-coated carrier. This finding suggests that, even though the polymeric coating helps preventing excessive release and volatilization of the AI from the carrier, it slightly enhances mobility compared to bare K10 particles. However, in the second part of the transport tests (PVs 10 to 20), when the columns were flushed with DIw, the abrupt change in ionic strength generated a markedly different response of bare and CMC-coated carriers. The uncoated nano-formulation was strongly mobilized by the step change in ionic strength, resulting in the remobilization of most formulation previously retained in the column (79.68% of the K10 carrier and 88.43% or the total injected dicamba was eluted at the end of the test). Conversely, the

528 mobilization of the CMC-coated nano-formulation was minimal, resulting in in an overall elution of 15.35%
529 of the injected carrier, corresponding to 24.52% of the total injected dicamba. This last finding remarkably
530 suggests that, even though the CMC coating imparts a slightly higher mobility to the nano-formulation, it also
531 reduces the effects of changes in ionic strength. In particular, it decreases the possibility of the retained nano-
532 formulation re-mobilization in case the salt concentration is reduced, for example, due to intense infiltration
533 of rain.

534

535 3.5. Weed control efficacy tests

536 The dose-response curve highlighted a relative weight reduction of the treated weeds at increasing herbicide
537 rates (Figure 6 and Table S2 in Supporting Information). All the herbicide formulations showed higher efficacy
538 on S. *nigrum* than against *A*. *retroflexus*. However, the efficacy was consistent between herbicides in the two
539 species, highlighting a higher relative weight reduction with K10-CMC, followed by commercial dicamba and
540 K10. The herbicide rate able to reduce weed biomass by 50% showed higher differences between herbicides
541 with K10-CMC always displaying the lowest rates: 1.5 g AI/ha for S. *nigrum* and 33 g AI/ha for *A*. *retroflexus*.
542 At 90% weight reduction (corresponding to a relative weight of 10% in comparison to control) all the
543 herbicides acted similarly, particularly in the case of *A*. *retroflexus*, in which values of herbicide rates higher
544 than 100 g AI/ha were necessary to obtain a similar efficacy level. In the case of *S*. *nigrum,* 90% weight
545 reduction was obtained at about 50 g AI/ha, value much smaller than that required for commercial and K10.

546

547 4. CONCLUSIONS

548 In this work a novel approach based on the use of natural clays to reduce the environmental mobility of
549 dicamba was proposed. Four candidate carriers (namely, two Na-montmorillonites, a Ca-montmorillonite
550 and a zeolite) were tested, and all proved to be effective in adsorbing the herbicide. However, not all of them

551 guaranteed easy applicability or reduced release in water when the formulations were diluted (i.e. mimicking
552 the preparation of the product prior field application). A key role was played by the polymeric coating, formed
553 by carboxymethyl cellulose, a food-grade biodegradable polymer used in a broad range of applications, from
554 food industry to enhanced oil recovery to pharmaceutics. The best performing formulation, namely CMC-
555 coated Na-montmorillonite K10, was identified as the most advantageous compromise between technical
556 constraints and potential environmental effects. From the technical point of view, it showed a good control
557 of dicamba release after dilution and good colloidal stability, which allows its application using conventional
558 pesticide spraying equipment. Its efficacy in the greenhouse tests against target weeds was similar or
559 sometimes higher than that of commercial dicamba formulation, and showed promising prospects for
560 improvements, which will be the focus of upcoming work.

561 Compared to other approaches previously proposed in the literature, based on organoclays and, more in
562 general, of chemically modified adsorbing carriers, in this work the focus was on the use of natural
563 unmodified materials as carriers, and on the development of a simple and low-impact preparation method,
564 applicable at room temperature and pressure without addition of chemicals. The loading capacity obtained
565 in this study is comparable or lower than those reported in the literature for organoclays (e.g. (Carrizosa et
566 al., 2001)), but the CMC-coated K10 showed a good control of the major environmental criticalities of
567 dicamba, namely volatilization and mobility in the subsoil. In particular, the CMC-coated K10 allowed a
568 control of volatilization losses comparable to a commercial dicamba-based product, even in the absence of
569 specific co-formulants, which are present in the commercial formulation but were not included in the nano-
570 formulations.

571 Concerning the mobility in the subsoil, in this work a preliminary assessment was performed focusing on the
572 saturated zone, a potential major route for dicamba migration in the subsoil. The remarkable mobility of pure
573 and commercially formulated dicamba observed in transport tests, both in synthetic and real water indicates
574 that, in case dicamba reaches an aquifer system as a free compound, it is expected to be highly mobile
575 without any significant attenuation (except obviously for degradation processes, which are not appreciable
576 on the short time scale of the experiments performed in this study). Conversely, the use of a mineral carrier

significantly reduced the potential mobility, in all explored conditions. Also in this case, the polymeric coating played a key role. Even though it imparted a slightly higher mobility to the nano-formulations, compared to bare carriers, it also significantly reduced the risk of re-mobilization when abrupt hydrochemical perturbations were applied, namely, when the columns were flushed with deionized water. Even if this condition is clearly unrealistic in a field-scale scenario, it has been adopted here as an extremized simulation of intense rain events: in this case the precipitation, characterized by a significantly lower salinity than groundwater, may infiltrate and, particularly for shallow aquifer systems, can significantly reduce the local groundwater salinity, with the risk of local re-mobilization of the nano-formulation. Clearly an in-depth study of the potential mobility of the new nano-formulations in the subsoil requires the assessment of a broader range of experimental conditions, and a detailed investigation focused on the top soil, which is beyond the scope of this paper. More in general, deeper investigation is needed on several other aspects touched in this work, including for example a further optimization of the preparation procedure, and a more detailed evaluation of the nano-formulation efficacy toward target weeds. However, the authors believe that even the preliminary results presented here already provide a first insight on the potentialities of natural clays as a low-impact solution to reduce environmental drawbacks of critical agrochemicals.

5. CITED LITERATURE

Adisa IO, Pullagurala VLR, Peralta-Videa JR, Dimkpa CO, Elmer WH, Gardea-Torresdey JL, et al. Recent advances in nano-enabled fertilizers and pesticides: a critical review of mechanisms of action. Environmental Science: Nano 2019; 6: 2002-2030.

Aktar MW, Sengupta D, Chowdhury A. Impact of pesticides use in agriculture: their benefits and hazards. Interdisciplinary toxicology 2009; 2: 1-12.

Arias-Estévez M, López-Periago E, Martínez-Carballo E, Simal-Gándara J, Mejuto J-C, García-Río L. The mobility and degradation of pesticides in soils and the pollution of groundwater resources. Agriculture, Ecosystems & Environment 2008; 123: 247-260.

Authority EFS. Conclusion on the peer review of the pesticide risk assessment of the active substance dicamba. EFSA Journal 2011; 9: 1965.

Azeem B, KuShaari K, Man ZB, Basit A, Thanh TH. Review on materials & methods to produce controlled release coated urea fertilizer. Journal of Controlled Release 2014; 181: 11-21.

Azejjel H, del Hoyo C, Draoui K, Rodríguez-Cruz MS, Sánchez-Martín MJ. Natural and modified clays from Morocco as sorbents of ionizable herbicides in aqueous medium. Desalination 2009; 249: 1151-1158.

610 Behin J, Sadeghi N. Utilization of waste lignin to prepare controlled-slow release urea. International Journal
611 of Recycling of Organic Waste in Agriculture 2016; 5: 289-299.
612 Behrens MR, Mutlu N, Chakraborty S, Dumitru R, Jiang WZ, LaVallee BJ, et al. Dicamba Resistance: Enlarging
613 and Preserving Biotechnology-Based Weed Management Strategies. Science 2007; 316: 1185-1188.
614 Bianco C, Tosco T, Sethi R. A 3-dimensional micro- and nanoparticle transport and filtration model (MNM3D)
615 applied to the migration of carbon-based nanomaterials in porous media. Journal of Contaminant
616 Hydrology 2016; 193: 10-20.
617 Bongiovanni R, Lowenberg-Deboer J. Precision agriculture and sustainability. Precision Agriculture 2004; 5:
618 359-387.
619 Boutin C, Strandberg B, Carpenter D, Mathiassen SK, Thomas PJ. Herbicide impact on non-target plant
620 reproduction: What are the toxicological and ecological implications? Environmental Pollution
621 2014; 185: 295-306.
622 Bueno V, Ghoshal S. Self-Assembled Surfactant-Templated Synthesis of Porous Hollow Silica Nanoparticles:
623 Mechanism of Formation and Feasibility of Post-Synthesis Nanoencapsulation. Langmuir 2020; 36:
624 14633-14643.
625 Cabrera A, Celis R, Hermosín MC. Imazamox–clay complexes with chitosan- and iron(III)-modified smectites
626 and their use in nanoformulations. Pest Management Science 2016; 72: 1285-1294.
627 Carrizosa MJ, Koskinen WC, Hermosin MC, Cornejo J. Dicamba adsorption–desorption on organoclays.
628 Applied Clay Science 2001; 18: 223-231.
629 Celis R, Hermosín MC, Carrizosa MJ, Cornejo J. Inorganic and Organic Clays as Carriers for Controlled Release
630 of the Herbicide Hexazinone. Journal of Agricultural and Food Chemistry 2002; 50: 2324-2330.
631 Cornejo L, Celis R, Domínguez C, Hermosín MC, Cornejo J. Use of modified montmorillonites to reduce
632 herbicide leaching in sports turf surfaces: Laboratory and field experiments. Applied Clay Science
633 2008; 42: 284-291.
634 Cox L, Celis R, Hermosín MC, Cornejo J. Natural Soil Colloids To Retard Simazine and 2,4-D Leaching in Soil.
635 Journal of Agricultural and Food Chemistry 2000; 48: 93-99.
636 da Costa TP, Westphalen G, Nora FBD, de Zorzi Silva B, Rosa GSd. Technical and environmental assessment
637 of coated urea production with a natural polymeric suspension in spouted bed to reduce nitrogen
638 losses. Journal of Cleaner Production 2019; 222: 324-334.
639 Damalas CA, Eleftherohorinos IG. Pesticide exposure, safety issues, and risk assessment indicators.
640 International Journal of Environmental Research and Public Health 2011; 8: 1402-1419.
641 Dayan FE, Cantrell CL, Duke SO. Natural products in crop protection. Bioorganic and Medicinal Chemistry
642 2009; 17: 4022-4034.
643 Dimkpa CO, Fugice J, Singh U, Lewis TD. Development of fertilizers for enhanced nitrogen use efficiency –
644 Trends and perspectives. Science of The Total Environment 2020; 731: 139113.
645 Ding G, Guo D, Zhang W, Han P, Punyapitak D, Guo M, et al. Preparation of novel auxinic herbicide derivatives
646 with high-activity and low-volatility by me-too method. Arabian Journal of Chemistry 2019; 12:
647 4707-4718.
648 Egan JF, Mortensen DA. Quantifying vapor drift of dicamba herbicides applied to soybean. Environmental
649 Toxicology and Chemistry 2012; 31: 1023-1031.
650 Elhaj Baddar Z, Gurusamy D, Laisney J, Tripathi P, Palli SR, Unrine JM. Polymer-Coated Hydroxyapatite
651 Nanocarrier for Double-Stranded RNA Delivery. Journal of Agricultural and Food Chemistry 2020;
652 68: 6811-6818.
653 Elimelech M. Particle deposition and aggregation : measurement, modelling, and simulation. Oxford
654 [England] ; Boston: Butterworth-Heinemann, 1995.
655 European Commission. EU Pesticides database. https://ec.europa.eu/food/plant/pesticides/eu-pesticides-
656 db_en, 2021.
657 EUROSTAT. Agri-environmental indicator - pesticide pollution of water November 2017.
658 Fogliatto S, Patrucco L, Milan M, Vidotto F. Sensitivity to salinity at the emergence and seedling stages of
659 barnyardgrass (Echinochloa crus-galli), weedy rice (Oryza sativa), and rice with different tolerances
660 to ALS-inhibiting herbicides. Weed Science 2021; 69: 39-51.

661 Gao Y, Xiao Y, Mao K, Qin X, Zhang Y, Li D, et al. Thermoresponsive polymer-encapsulated hollow mesoporous
662 silica nanoparticles and their application in insecticide delivery. Chemical Engineering Journal 2020;
663 383: 123169.
664 Gomes SIL, Scott-Fordsmand JJ, Campos EVR, Grillo R, Fraceto LF, Amorim MJB. On the safety of
665 nanoformulations to non-target soil invertebrates – an atrazine case study. Environmental Science:
666 Nano 2019; 6: 1950-1958.
667 Hermosin MC, Calderón MJ, Aguer J-P, Cornejo J. Organoclays for controlled release of the herbicide fenuron.
668 Pest Management Science 2001; 57: 803-809.
669 Iavicoli I, Leso V, Beezhold DH, Shvedova AA. Nanotechnology in agriculture: Opportunities, toxicological
670 implications, and occupational risks. Toxicology and Applied Pharmacology 2017; 329: 96-111.
671 Joshi PP, Van Cleave A, Held DW, Howe JA, Auad ML. Preparation of slow release encapsulated insecticide
672 and fertilizer based on superabsorbent polysaccharide microbeads. Journal of Applied Polymer
673 Science 2020; 137: 49177.
674 Kah M, Hofmann T. Nanopesticide research: Current trends and future priorities. Environment International
675 2014; 63: 224-235.
676 Kah M, Kookana RS, Gogos A, Bucheli TD. A critical evaluation of nanopesticides and nanofertilizers against
677 their conventional analogues. Nature Nanotechnology 2018a; 13: 677-684.
678 Kah M, Tufenkji N, White JC. Nano-enabled strategies to enhance crop nutrition and protection. Nature
679 Nanotechnology 2019; 14: 532-540.
680 Kah M, Walch H, Hofmann T. Environmental fate of nanopesticides: durability, sorption and
681 photodegradation of nanoformulated clothianidin. Environmental Science: Nano 2018b; 5: 882-
682 889.
683 Kenawy E-R, Sakran MA. Controlled Release Formulations of Agrochemicals from Calcium Alginate. Industrial
684 & Engineering Chemistry Research 1996; 35: 3726-3729.
685 Kök FN, Arıca MY, Gencer O, Abak K, Hasırcı V. Controlled release of aldicarb from carboxymethyl cellulose
686 microspheres: in vitro and field applications. Pesticide Science 1999; 55: 1194-1202.
687 Lamberth C, Jeanmart S, Luksch T, Plant A. Current challenges and trends in the discovery of agrochemicals.
688 Science 2013; 341: 742-746.
689 Lapworth DJ, Gooddy DC, Stuart ME, Chilton PJ, Cachandt G, Knapp M, et al. Pesticides in groundwater: some
690 observations on temporal and spatial trends. Water and Environment Journal 2006; 20: 55-64.
691 Luna M, Gastone F, Tosco T, Sethi R, Velimirovic M, Gemoets J, et al. Pressure-controlled injection of guar
692 gum stabilized microscale zerovalent iron for groundwater remediation. Journal of Contaminant
693 Hydrology 2015; 181: 46-58.
694 Mondino F, Piscitello A, Bianco C, Gallo A, de Folly D'Auris A, Tosco T, et al. Injection of zerovalent iron gels
695 for aquifer nanoremediation: Lab experiments and modeling. Water (Switzerland) 2020; 12: 1-15.
696 Moulick RG, Das S, Debnath N, Bandyopadhyay K. Potential use of nanotechnology in sustainable and 'smart'
697 agriculture: advancements made in the last decade. Plant Biotechnology Reports 2020; 14: 505-
698 513.
699 Mueller TC. Methods To Measure Herbicide Volatility. Weed Science 2015; 63: 116-120.
700 Nuruzzaman M, Ren J, Liu Y, Rahman MM, Shon HK, Naidu R. Hollow Porous Silica Nanosphere with Single
701 Large Pore Opening for Pesticide Loading and Delivery. ACS Applied Nano Materials 2020; 3: 105-
702 113.
703 Oliveira Jr RS, Koskinen WC, Ferreira FA. Sorption and leaching potential of herbicides on Brazilian soils. Weed
704 Research 2001; 41: 97-110.
705 Petosa AR, Rajput F, Selvam O, Öhl C, Tufenkji N. Assessing the transport potential of polymeric nanocapsules
706 developed for crop protection. Water Research 2017; 111: 10-17.
707 Pimentel D. Pesticides and pest control. Integrated Pest Management. 1, 2009, pp. 83-87.
708 Rashidzadeh A, Olad A, Hejazi MJ. Controlled Release Systems Based on Intercalated Paraquat onto
709 Montmorillonite and Clinoptilolite Clays Encapsulated with Sodium Alginate. Advances in Polymer
710 Technology 2017; 36: 177-185.

711 Reichenberger S, Bach M, Skitschak A, Frede HG. Mitigation strategies to reduce pesticide inputs into ground-
712 and surface water and their effectiveness; A review. Science of the Total Environment 2007; 384:
713 1-35.
714 Rhodes CJ. Properties and applications of zeolites. Sci Prog 2010; 93: 223-84.
715 Riggi E, Santagata G, Malinconico M. Bio-based and biodegradable plastics for use in crop production. Recent
716 Patents on Food, Nutrition & Agriculture 2011; 3: 49-63.
717 Sakaliene O, Papiernik SK, Koskinen WC, Spokas KA. Sorption and predicted mobility of herbicides in Baltic
718 soils. Journal of Environmental Science and Health, Part B 2007; 42: 641-647.
719 Sanchez-Bayo F, Goka K. Pesticide Residues and Bees – A Risk Assessment. PLOS ONE 2014; 9: e94482.
720 Sciumbato AS, Chandler JM, Senseman SA, Bovey RW, Smith KL. Determining Exposure to Auxin-Like
721 Herbicides. I. Quantifying Injury to Cotton and Soybean. Weed Technology 2004; 18: 1125-1134.
722 Servin A, Elmer W, Mukherjee A, De la Torre-Roche R, Hamdi H, White JC, et al. A review of the use of
723 engineered nanomaterials to suppress plant disease and enhance crop yield. Journal of
724 Nanoparticle Research 2015; 17: 92.
725 Shasha BS, Doane WM, Russell CR. Starch-encapsulated pesticides for slow release. Journal of Polymer
726 Science: Polymer Letters Edition 1976; 14: 417-420.
727 Silva V, Mol HGJ, Zomer P, Tienstra M, Ritsema CJ, Geissen V. Pesticide residues in European agricultural soils
728 – A hidden reality unfolded. Science of the Total Environment 2019; 653: 1532-1545.
729 Singh H, Sharma A, Bhardwaj SK, Arya SK, Bhardwaj N, Khatri M. Recent advances in the applications of nano-
730 agrochemicals for sustainable agricultural development. Environmental Science: Processes &
731 Impacts 2021; 23: 213-239.
732 Sopeña F, Maqueda C, Morillo E. Controlled release formulations of herbicides based on micro-encapsulation.
733 Ciencia e Investigacion Agraria 2009; 36: 27-42.
734 Stocker K, Ellersdorfer M, Lehner M, Raith JG. Characterization and Utilization of Natural Zeolites in Technical
735 Applications. BHM Berg- und Hüttenmännische Monatshefte 2017; 162: 142-147.
736 Strachan SD, Casini MS, Heldreth KM, Scocas JA, Nissen SJ, Bukun B, et al. Vapor Movement of Synthetic
737 Auxin Herbicides: Aminocyclopyrachlor, Aminocyclopyrachlor-Methyl Ester, Dicamba, and
738 Aminopyralid. Weed Science 2010; 58: 103-108.
739 Team\ RDC. R: A Language and Environment for Statistical Computing. Vienna, Austria: R Foundation for
740 Statistical Computing. , 2019.
741 Tindall JA, Vencill WK. Transport of atrazine, 2,4-D, and dicamba through preferential flowpaths in an
742 unsaturated claypan soil near Centralia, Missouri. Journal of Hydrology 1995; 166: 37-59.
743 Tosco T, Sethi R. Transport of Non-Newtonian Suspensions of Highly Concentrated Micro- And Nanoscale Iron
744 Particles in Porous Media: A Modeling Approach. Environmental Science & Technology 2010; 44:
745 9062-9068.
746 Usman M, Farooq M, Wakeel A, Nawaz A, Cheema SA, Rehman Hu, et al. Nanotechnology in agriculture:
747 Current status, challenges and future opportunities. Science of the Total Environment 2020; 721:
748 137778.
749 van den Berg F, Kubiak R, Benjey WG, Majewski MS, Yates SR, Reeves GL, et al. Emission of Pesticides into
750 the Air. Water, Air, and Soil Pollution 1999; 115: 195-218.
751 Velimirovic M, Bianco C, Ferrantello N, Tosco T, Casasso A, Sethi R, et al. A Large-Scale 3D Study on Transport
752 of Humic Acid-Coated Goethite Nanoparticles for Aquifer Remediation. Water 2020; 12: 1207.
753 Wauchope RD. The Pesticide Content of Surface Water Draining from Agricultural Fields—A Review. Journal
754 of Environmental Quality 1978; 7: 459-472.
755 Worrall EA, Hamid A, Mody KT, Mitter N, Pappu HR. Nanotechnology for Plant Disease Management.
756 Agronomy 2018; 8: 285.
757 Xu S, Gao B, Saiers JE. Straining of colloidal particles in saturated porous media. Water Resources Research
758 2006; 42.

759

760

Conflicts of interest

There are no conflicts to declare

Acknowledgements

This work was supported by the project Nanograss co-funded by Compagnia di San Paolo. The authors also wish to thank Sofia Credaro for the support in the manuscript proofreading.

Figures

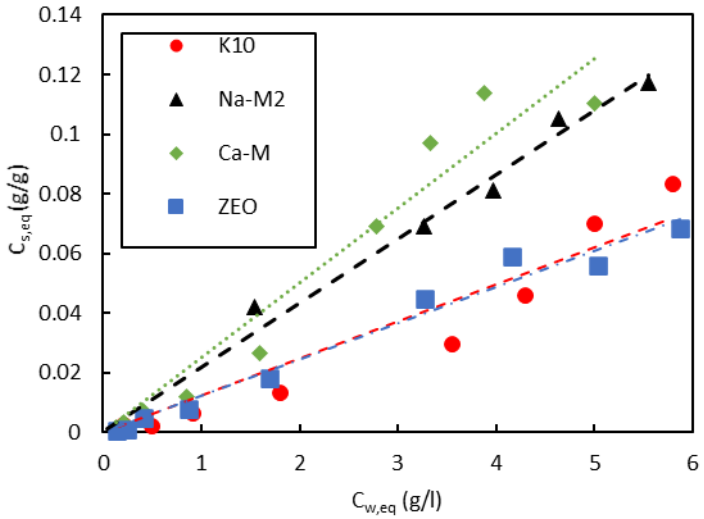

Figure 1 Adsorption isotherms for the four candidate carriers (K10, Na-M2, Ca-M, ZEO) obtained for a contact time of 24 hours. Experimental data (dots) and least-squares fitted linear isotherms (lines).

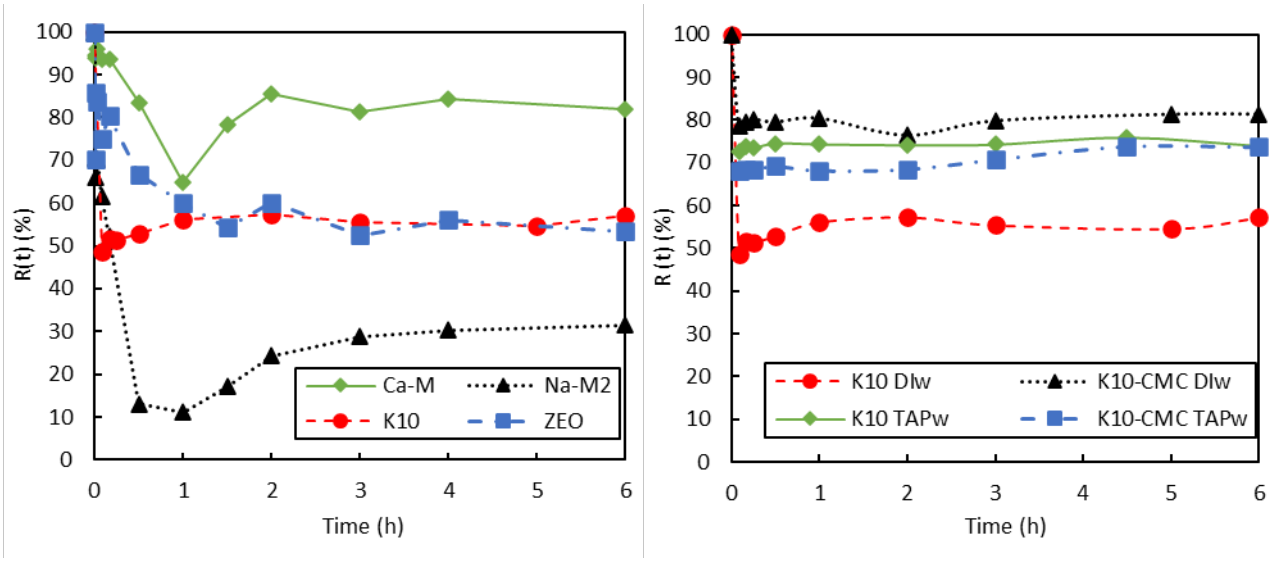

(a) (b)

Figure 2 Release tests: retained dicamba R(t) expressed as a percentage for the four carriers (ZEO, Na-M2, Ca-M, ZEO), after dilution in deionized water (DIw), without CMC coating (a), and on K10, after dilution in deionized water (DIw) or in tap water (TAPw), with and without CMC coating (b)

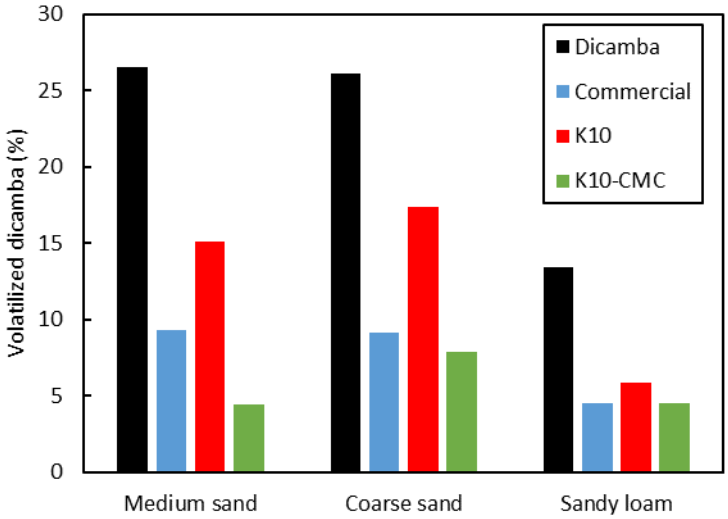

780

781 *Figure 3 Volatilization from soils: dicamba loss 24 h after application to different soils, reported as percentage of*
782 *volatilized mass with respect to applied mass*

783

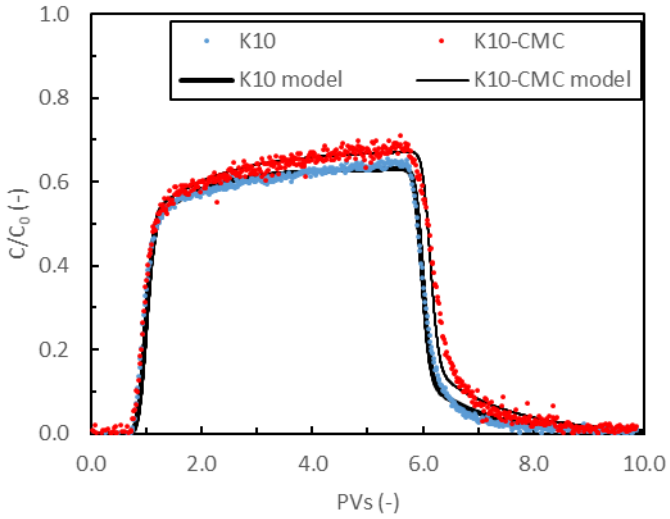

784

785 *Figure 4: Breakthrough curves for uncoated (blue) and CMC-coated (red) K10 carrier, without dicamba. Experimental*
786 *data (coloured dots) and least-squares model curves (black lines) are reported.*

787

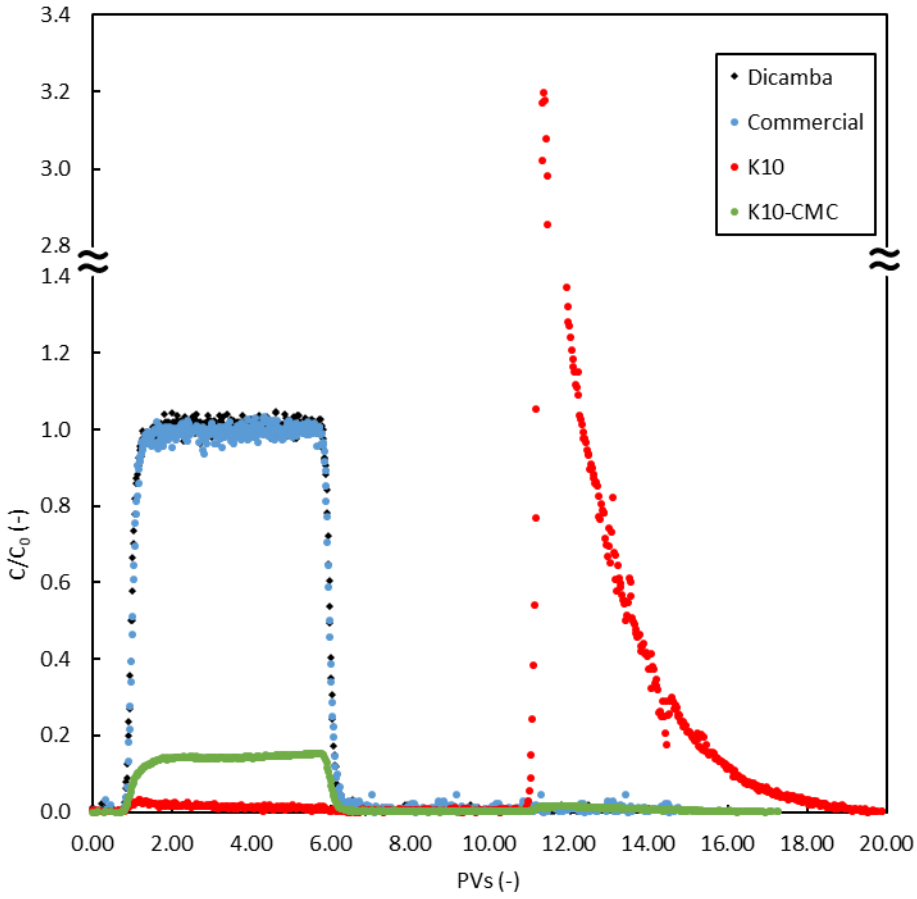

Figure 5 Breakthrough curves for non-formulated dicamba (black), commercial formulation (blue), uncoated (red) and CMC-coated (green) nano-formulations. All formulations were dispersed in NaCl 30 mM solution (injection: pore volumes 0 to 5); the first flushing (pore volumes 5 to 10) was performed injecting pesticide-free 30 mM NaCl solution; the second flushing (pore volumes 10 to 20) was performed with DIw.

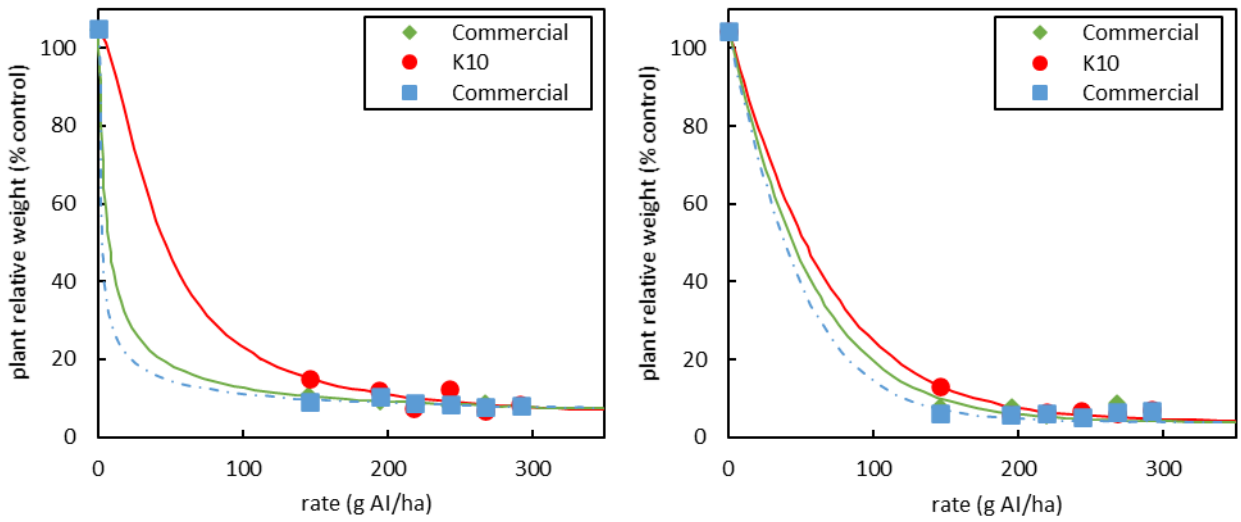

(a) (b)

Figure 6 Dose-response curves between Solanum nigrum (a) and Amaranthus retroflexus (b) plant relative weight and herbicide dose of K10-CMC, commercial dicamba and K10 formulations.

Tables

Table 1 Size and zeta potential in DIW and their variation in NaCl different ionic strength

	Particle size distribution (μm)				Zeta potential (mV)		
	D_{10}	D_{50}	D_{90}	$U=D_{60}/D_{10}$	in DIW	in NaCl 100 mM	in $CaCl_2$ 2mM
K10	0.287	1.561	3.746	6.49	-18.9 ± 2.0	-14.2 ± 0.7	-6.2 ± 0.5
Na-M2	0.154	0.570	2.834	6.06	-26.5 ± 2.6	-14.6 ± 2.8	-13.2 ± 1.1
Ca-M	0.180	0.656	2.262	4.93	-14.3 ± 0.9	-10.2 ± 0.1	-8.0 ± 0.6
ZEO	0.674	2.525	2.525	4.39	-18.2 ± 0.5	-8.7 ± 0.3	-12.3 ± 1.0

Table 2 Mass balance and fitted model parameters for the transport of carriers and formulations in the porous medium

			K10 carrier only		Dicamba formulations			
			K10	**K10-CMC**	**Dicamba**	**Commercial**	**K10**	**K10-CMC**
Mass balance	Carrier	Eluted mass @10 PVs	63.09%	67.22%	n.a.	n.a.	1.74%	14.45%
		Eluted mass @20 PVs	n.a.	n.a.	n.a.	n.a.	79.68%	15.35%
	Free dicamba	Eluted mass @10 PVs	n.a.	n.a.	99.35%	98.44%	99.77%	100.00%
	Total dicamba	Eluted mass @10 PVs	n.a.	n.a.	99.35%	98.44%	10.06%	20.73%
		Eluted mass @20 PVs	n.a.	n.a.	n.a.	n.a.	88.43%	24.52%
Modeling	Site 1	$k_{a,1}$ (1/s)	$6.99\cdot10^{-4}$	$6.32\cdot10^{-4}$	n.a.	n.a.	$4.00\cdot10^{-3}$	$4.48\cdot10^{-3}$
	Site 2	$k_{a,2}$ (1/s)	$3.53\cdot10^{-4}$	$4.32\cdot10^{-4}$	n.a.	n.a.	$6.40\cdot10^{-3}$	$9.70\cdot10^{-4}$
		$k_{d,2}$ (1/s)	$1.68\cdot10^{-3}$	$1.38\cdot10^{-3}$	n.a.	n.a.	$2.68\cdot10^{-5}$	$6.07\cdot10^{-3}$
		A_2 (-) (*)	0	0	n.a.	n.a.	998.1	0
		β_2 (-) (**)	1	1	n.a.	n.a.	1	1
	Fitting	R^2	0.9963	0.9937	n.a.	n.a.	0.8384	0.9956

(*) fitted only for dicamba nano-formulations

(**) not fitted

Declaration of interests

☒ The authors declare that they have no known competing financial interests or personal relationships that could have appeared to influence the work reported in this paper.

☐The authors declare the following financial interests/personal relationships which may be considered as potential competing interests: